

Straining of a polycrystal of Fe–Pd with martensite structure by uniaxial loading

Yuanchang Liang, Taishi Wada, Hiroyuki Kato¹, Tetsuya Tagawa², Minoru Taya*, T. Mori

Department of Mechanical Engineering, Center for Intelligent Materials and Systems, University of Washington, Box 352600, Seattle, WA 98195-2600, USA

Received 28 August 2001; received in revised form 8 January 2002

Abstract

This paper proposes a method to calculate the uniaxial stress–strain relationship of polycrystalline Fe–Pd, which has a martensite structure produced by cooling. Strain is caused by changes in the fractions of the three Bain corresponding variants which form the martensite structure within each grain. Internal stress and elastic energy are accumulated as straining proceeds and are caused by differences of eigenstrain (transformation strain) between differently oriented grains. The stress and elastic energy are evaluated on the basis of micromechanics. The stress acting on a grain due to surrounding grains is calculated using a mean field method. In this procedure, an averaging method is introduced, by which the mean field of grains having the same tensile direction, but having random lateral directions, are written in a closed form. The averaging method facilitates computations. It is shown that tension and compression differ in the stress–strain relationship. © 2002 Elsevier B.V. All rights reserved.

Keywords: Ferromagnetic shape memory alloys; Stress–strain curve; Bain corresponding variants; Fe–Pd; Martensite transformation

1. Introduction

As reported previously, polycrystalline Fe–Pd has low stiffness in the martensite state [1]. In addition to intrinsically low lattice stiffness, large strains are developed upon loading due to changes in martensite variant fractions. This makes polycrystalline Fe–Pd a softer material, suitable for certain actuator applications. The structure of martensite in a polycrystal of Fe–Pd has been analyzed on the basis of elasticity [2]. Three Bain correspondence variants of tetragonal martensite, BCV(1), BCV(2) and BCV(3), exist in Fe–Pd. Here, the number in the parentheses denotes the direction of the *c*-axis of a variant with respect to the parent cubic phase. When formed by cooling alone, a grain has a

structure consisting of alternating dark and bright plates, as observed under optical microscopy [2]. The width of the plates is a few μm . Each plate has a fine structure, in which two twin-related BCVs are alternately stacked together. A BCV is about 50 nm thick. Their interfaces are $\{110\}$, as observed by electron microscopy [2]. The interfaces of the dark and bright plates are also $\{110\}$. An example of this structure is illustrated in Fig. 1, in which a plate (e.g. a bright plate) consisting of BCV(1) and BCV(2) abuts on another plate (e.g. a dark plate) consisting of BCV(3) and BCV(2). When stressed, the fractions of BCVs change by movement of the interfaces, resulting in straining of the polycrystal. The variant change depends on the orientation of a grain and the constraint imposed by the surrounding grains.

The constraint imposed by surrounding grains makes the stress–strain relationship different from that of a single crystal. Since polycrystalline Fe–Pd is likely to be used for actuator applications, the determination of this relationship is a key engineering issue. This also applies to straining due to variant changes caused by the application of a magnetic field. James and Wuttig [3]

* Corresponding author. Tel.: +1-206-685-2850; fax: +1-206-685-8047.

E-mail address: tayam@u.washington.edu (M. Taya).

¹ Present address: Department of Mechanical Engineering, Hokkaido University, 060-8628, Japan.

² Present address: Department of Materials Science and Engineering, Nagoya University, 464-8603, Japan.

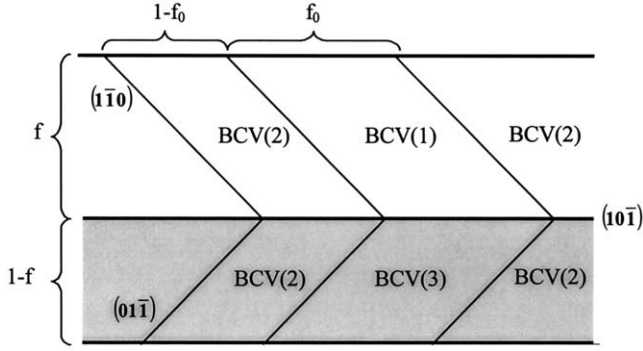


Fig. 1. Martensite structure in Fe–Pd. BCV(1), BCV(2) and BCV(3) are the variants having the c -axis parallel to the austenite [100], [010] and [001], respectively.

and Koeda, Nakamura, Fukuda, Kakeshita, Takeuchi and Kishio [4] have reported that when a magnetic field is applied across a single crystal in the martensite state, large strains are induced. The strains are in the order of 0.1%. However, when a polycrystal is used, only a strain of 0.01% is observed, even under a field of 10 kG [5]. This small strain is partly due to the constraint mentioned above. The origin of larger strain of the order of 0.1% reported by Furuya et al. in polycrystalline Fe–Pd, [6–8], will be discussed later.

This paper presents a method to calculate the above mentioned variant change and straining under uniaxial loading of a fully martensite Fe–Pd, using the mean field method [9,10]. The stress state and elastic energy are also given.

2. Analysis

From our previous paper [2], the average transformation strain (eigenstrain) in a grain that has the a structure shown in Fig. 1 is written as:

$$\varepsilon^*(Y) = \frac{2\varepsilon_a + \varepsilon_c}{3} \begin{pmatrix} 1 & 0 & 0 \\ 0 & 1 & 0 \\ 0 & 0 & 1 \end{pmatrix} - (\varepsilon_a - \varepsilon_c) \times \begin{pmatrix} f_1 - 1/3 & 0 & 0 \\ 0 & f_2 - 1/3 & 0 \\ 0 & 0 & f_3 - 1/3 \end{pmatrix} \quad (1)$$

Here, $\varepsilon_a = (a - a_0)/a_0$ and $\varepsilon_c = (c - a_0)/a_0$. a_0 is the lattice parameter of the cubic austenite phase and a and c are, respectively, the lattice parameters of the a -axis and c -axis of the tetragonal martensite phase, $f_1 = f \cdot f_0$ is the volume fraction of BCV(1), $f_2 = (1 - f) \cdot f_0$ that of BCV(2) and $f_3 = (1 - f) \cdot f_0$ that of BCV(3). f and f_0 refer to Fig. 1. The eigenstrain in Eq. (1) refers to the coordinate system (Y) with axes parallel to the crystallographic directions, [100], [010] and [001], in the austenite. The first term in Eq. (1) is common among all grains and causes no internal stress. Thus, it is

omitted in the following analysis. The second term is rewritten as:

$$\varepsilon^*(Y) = -\beta \begin{pmatrix} f_1^* & 0 & 0 \\ 0 & f_2^* & 0 \\ 0 & 0 & f_3^* \end{pmatrix} \quad (2)$$

where:

$$\beta = \varepsilon_a - \varepsilon_c \quad (3)$$

and,

$$f_1^* = f_1 - \frac{1}{3}, \quad f_2^* = f_2 - \frac{1}{3}, \quad f_3^* = f_3 - \frac{1}{3}, \quad (4)$$

f_1^* is the deviation of the fraction of BCV(I) from the average of 1/3. One third is the value taken by all BCVs after transformation by cooling below M_s [2]. It is this deviation, due to variant changes, which causes straining during loading f_i^* s satisfy

$$f_1^* + f_2^* + f_3^* = 0 \quad (5)$$

Our task here is to evaluate the internal stresses and elastic energy in polycrystalline Fe–Pd, in which many differently oriented grains exist and undergo variant changes depending on their orientations. We consider uniaxial loading. The specimen coordinate reference frame is denoted as X , x_3 being parallel to the loading direction. To facilitate the calculation, the grains are grouped into N groups. All grains belonging to the same group, say the I -th group, have the same crystallographic direction along the loading direction. This direction has a unit vector $l(1)$. The lateral directions of these grains are random and axisymmetrically distributed around the loading direction. A polycrystal which possesses grains having many different orientations $l(1)$ is randomly oriented.

2.1. Stress due to grains in the I -th group

In the Y -coordinate (crystal axis coordinate) system, the stress in a grain belonging to the I -th group is written as:

$$\sigma^*(1, Y) = \alpha \beta \begin{pmatrix} f_1^*(I) & 0 & 0 \\ 0 & f_2^*(I) & 0 \\ 0 & 0 & f_3^*(I) \end{pmatrix}, \quad (6)$$

when only this grain changes its variant fractions [11]. Here, α is:

$$\alpha = 2\mu \frac{(7 - 5\nu)}{15(1 - \nu)} \quad (7)$$

The shape of a grain is assumed to be spherical, μ , is the shear modulus and ν the Poisson ratio. Isotropic elasticity is assumed. $\sigma^*(I, Y)$ is called the self-stress of a grain in the I -th group.

All the grains belonging to the same group should have identical f^* s and exert internal stress upon all other grains in the specimen. To calculate this internal stress, we proceed as follows. Eqs. (2) and (6) are written in the specimen coordinate (X -coordinate system) as:

$$\varepsilon^*(I, X) = -\beta \begin{pmatrix} \lambda_1(I) & \varepsilon_{12}^*(I) & \varepsilon_{13}^*(I) \\ \varepsilon_{21}^*(I) & \lambda_2(I) & \varepsilon_{23}^*(I) \\ \varepsilon_{31}^*(I) & \varepsilon_{32}^*(I) & \lambda_3(I) \end{pmatrix} \quad (8)$$

and,

$$\sigma^*(I, X) = \alpha\beta \begin{pmatrix} \lambda_1(I) & \varepsilon_{12}^*(I) & \varepsilon_{13}^*(I) \\ \varepsilon_{21}^*(I) & \lambda_2(I) & \varepsilon_{23}^*(I) \\ \varepsilon_{31}^*(I) & \varepsilon_{32}^*(I) & \lambda_3(I) \end{pmatrix} \quad (9)$$

[11]. Here,

$$\lambda_3(I) = f_1^*(I)(l_1(I))^2 + f_2^*(I)(l_2(I))^2 + f_3^*(I)(l_3(I))^2 \quad (10)$$

$$\lambda_1(I) + \lambda_2(I) + \lambda_3(I) = 0 \quad (11)$$

λ_3 is the tensile strain along this direction. ε_{12}^* etc. depend on $f_1^*(I)$, $f_2^*(I)$ and $f_3^*(I)$ and the exact orientation of the grain with respect to the loading direction.

Stress Eq. (9) is averaged over all the grains of the I -th group. As of the axi-symmetry around the x_3 -axis, the averages of the stresses due to the non-diagonal components in Eq. (9) vanish and the averages of the $\{1,1\}$ and $\{2,2\}$ components become the average of those components in Eq. (9), as will be shown in Appendix A. In this way, the average stress is written as:

$$\langle \sigma^*(I, X) \rangle_{V_0} = \alpha\beta \begin{pmatrix} (\lambda_1(I) + \lambda_2(I))/2 & 0 & 0 \\ 0 & (\lambda_1(I) + \lambda_2(I))/2 & 0 \\ 0 & 0 & \lambda_3(I) \end{pmatrix} \quad (12)$$

Here, V_0 stands for the volume of one grain. Eq. (12) is rewritten as:

$$\langle \sigma^*(I, X) \rangle_{V_0} = \alpha\beta \begin{pmatrix} -\lambda_3(I)/2 & 0 & 0 \\ 0 & -\lambda_3(I)/2 & 0 \\ 0 & 0 & \lambda_3(I) \end{pmatrix} \quad (13)$$

using Eq. (11). The grains in the I -th group cause average stress in the specimen given by [9,10]:

$$\bar{\sigma}(I, X) = -g(I) \langle \sigma^*(I, X) \rangle_{V_0} \quad (14)$$

Here $g(I)$ is the volume fraction of the grains belonging to the I -th group.

Similar equations are written for grains belonging to other groups. Thus, one grain belonging to the I -th group feels its self-stress plus the average stress from all other grains. The average stress is the sum of the forms given by Eq. (14) over all the groups. That is, the average stress is, in total,

$$\bar{\sigma}(X) = -g(J) \langle \sigma^*(J, X) \rangle_{V_0} \quad (15)$$

2.2. Elastic energy and total stress

Using the stress computed in the previous section, the elastic energy W per unit volume is calculated as:

$$\begin{aligned} W &= -\frac{1}{2} \sum_I g(I) \{ \sigma_{ij}^*(I) + \bar{\sigma}_{ij} \} \varepsilon_{ij}^*(I) \\ &= -\frac{1}{2} \sum_I g(I) \sigma_{ij}^*(I) \varepsilon_{ij}^*(I) - \frac{1}{2} \sum_I g(I) \varepsilon_{ij}^*(I, X) \\ &\quad \times \sum_J (-g(J)) \langle \sigma_{ij}^*(J, X) \rangle_{V_0} \end{aligned} \quad (16)$$

The first term is the self-energies, W_s , of all the grains and is calculated using the components expressed in the crystal coordinates. It is given by:

$$W_s = \frac{1}{2} \alpha\beta^2 \sum_I g(I) \{ (f_1^*(I))^2 + (f_2^*(I))^2 + (f_3^*(I))^2 \}, \quad (17)$$

using Eqs. (2) and (6). The second term in Eq. (16) is the interaction energy between the grains:

$$W_I = \frac{1}{2} \sum_I g(I) \varepsilon_{ij}^*(I, X) \sum_J (-g(J)) \langle \sigma_{ij}^*(J, X) \rangle_{V_0} \quad (18)$$

and is calculated using the components in the specimen coordinates. First, we obtain:

$$\begin{aligned} \varepsilon_{ij}^*(I, X) \sum_J (-g(J)) \langle \sigma_{ij}^*(J, X) \rangle_{V_0} \\ = \sum_J -g(J) \alpha\beta (-\beta) \\ \times \left\{ \frac{-\lambda_3(J)\lambda_1(I)}{2} - \frac{\lambda_3(J)\lambda_2(I)}{2} + \lambda_3(J)\lambda_3(I) \right\} \end{aligned} \quad (19)$$

from Eqs. (8) and (13). This is simplified to:

$$\begin{aligned} \varepsilon_{ij}^*(I, X) \sum_J (-g(J)) \langle \sigma_{ij}^*(J, X) \rangle_{V_0} \\ = \frac{3}{2} \alpha\beta^2 \lambda_3(I) \sum_J g(J) \lambda_3(J), \end{aligned} \quad (20)$$

using Eq. (11). Thus, W_I is given by:

$$\begin{aligned} W_I &= -\frac{3}{4} \alpha\beta^2 \left[\sum_I g(I) \right. \\ &\quad \times \{ f_1^*(I)(l_1(I))^2 + f_2^*(I)(l_2(I))^2 + f_3^*(I) \\ &\quad \times (l_3(I))^2 \} \left. \right]^2 \end{aligned} \quad (21)$$

using Eq. (10). The total elastic energy per unit volume is obtained from Eqs. (17) and (21) as:

$$\begin{aligned} W &= \frac{1}{2} \alpha\beta^2 \sum_I g(I) \{ (f_1^*(I))^2 + (f_2^*(I))^2 + (f_3^*(I))^2 \} \\ &\quad - \frac{3}{4} \alpha\beta [g(I) f_1^*(I)(l_1(I))^2 + f_2^*(I)(l_2(I))^2 + f_3^*(I) \\ &\quad \times (l_3(I))^2] \end{aligned} \quad (22)$$

The strain along the loading direction (x_3 -axis) is given by Eq. (10) as:

$$\varepsilon = -\beta \sum_I g(I) \times \{f_1^*(I)(l_1(I))^2 + f_2^*(I)(l_2(I))^2 + f_3^*(I)(l_3(I))^2\} \quad (23)$$

Thus, the potential energy, per unit volume, of the loading device is written as:

$$V = \sigma_0 \beta \sum_I g(I) \times \{f_1^*(I)(l_1(I))^2 + f_2^*(I)(l_2(I))^2 + f_3^*(I)(l_3(I))^2\} \quad (24)$$

where σ_0 is the uniaxial stress along the loading direction.

2.3. Stress–strain relationship

By ignoring the energy dissipation (friction), the stable condition of a specimen is found when $W+V$ (Gibbs free energy) is minimized:

$$\delta(W + V) = 0 \quad (25)$$

Eq. (25) results in a set of simultaneous linear equations in terms of $f_1^*(I)$, $f_2^*(I)$, and $f_3^*(I)$. Thus, all of $f_1^*(I)$, $f_2^*(I)$, and $f_3^*(I)$ are, in principle, obtained analytically as a function of the uniaxial stress σ_0 under the constraint of Eq. (5). Furthermore, $f_1^*(I)$, $f_2^*(I)$, and $f_3^*(I)$ must satisfy:

$$-\frac{1}{3} \leq f_1^* \leq \frac{2}{3} \quad (26)$$

$$-\frac{1}{3} \leq f_2^* \leq \frac{2}{3} \quad (27)$$

$$-\frac{1}{3} \leq f_3^* \leq \frac{2}{3} \quad (28)$$

Using Eq. (23), the strain ε along the loading direction attained under a uniaxial stress σ_0 is also obtained. Thus, the σ_0 versus ε relationship is com-

puted. Fig. 2 shows the case of four types of grains, the tensile directions of which are shown on the standard stereographic triangle in the insert. Each group of grains has volume fraction proportional to the solid angle indicated by its small triangle. Since energy dissipation is ignored, the variant change and the accompanied deformation proceed from $\sigma_0 = 0$. This is unrealistic and, thus, we will now take into account the energy dissipation.

2.4. Effect of energy dissipation on the movement of interfaces

Changes in the fractions of the martensite variants are produced by the movement of interfaces between them as seen in Fig. 1. Movement of the interfaces dissipates energy. Thus, extra work is supplied for straining. We will approximately evaluate the energy dissipation and incorporate it into the stress–strain relationship. We propose that the energy dissipation is calculated approximately as:

$$\delta W_D = \frac{k(|\delta f_1^*| + |\delta f_2^*| + |\delta f_3^*|)}{2} \quad (29)$$

per unit volume. k is the energy dissipation when a unit area of interface moves by a unit distance. The factor 2 is introduced to account for the fact that the movement of an interface changes the volumes of both variants which meet at the interface. Since this process is irreversible, we cannot use the energy minimization procedure to obtain the σ_0 versus ε relationship as adopted for the case of no energy dissipation. Thus, we simply add:

$$\sigma_D = \frac{\delta W_D}{\delta \varepsilon}, \quad (30)$$

to σ_0 determined without considering the energy dissipation. Here, $\delta \varepsilon$ is the increment of ε for the same change in the variant fractions. Since there is no unique way to determine k , we adopt the value which gives the initial stress for variant change, observed in our previous study [1,12]. One might argue that the adopted value, $k \sim 10^{-4} \mu$, is too small, since two variants match perfectly on their interface. However, Appendix B will show using a dislocation approach that the order of magnitude is correct.

In Fig. 3, the stress–strain diagrams with and without the energy dissipation are compared. In the computation, $\mu = 15$ GPa [1], $\nu = 0.33$ and $k = 2$ MPa are assumed. Also, $\beta = \varepsilon_a - \varepsilon_c = 2.54 \times 10^{-2}$ is used. This is based on the lattice parameters reported by Oshima [13]: $a_0 = 0.3750$ nm, $a = 0.3790$ nm and $a = 0.3695$ nm. As we expected, the energy dissipation just simply the stress level. Except for this change, no significant effect of the dissipation is seen in the σ_0 versus ε curve.

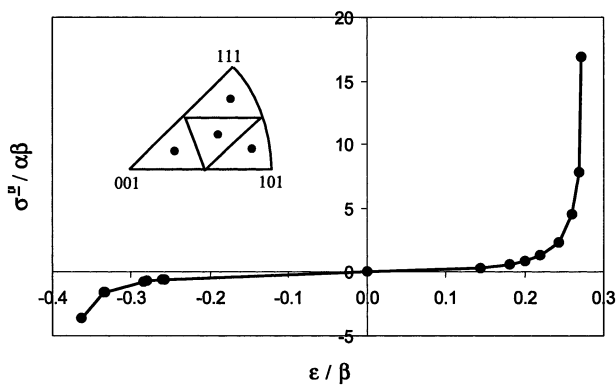


Fig. 2. Uniaxial stress–strain curve in a polycrystal having four types of grains. The directions of the grains are given in the insert. No energy dissipation for variant interface movement is taken into account.

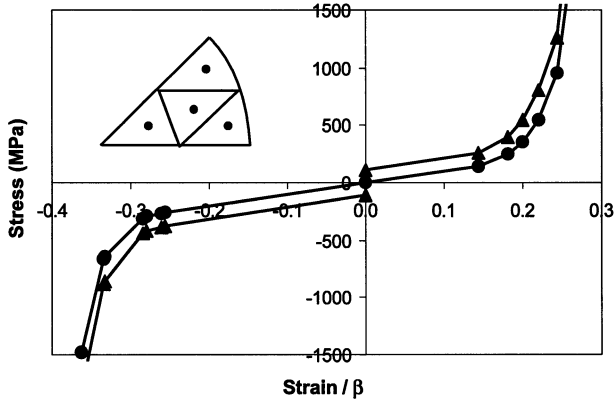


Fig. 3. Stress–strain curves of a polycrystal having four types of grains with (closed triangle) and without (closed circle) energy dissipation ($k = 2$ MPa).

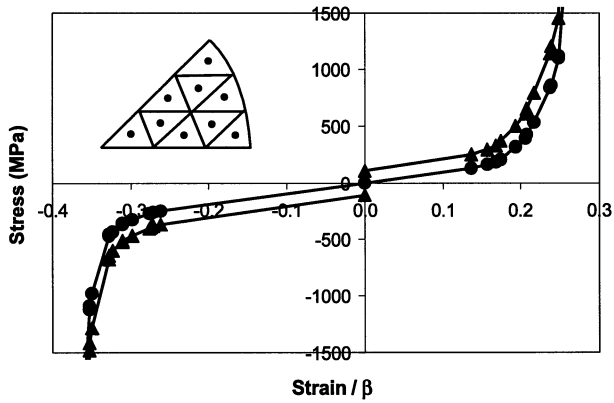


Fig. 4. Stress–strain curves of a polycrystal having nine types of grains with (closed triangle) and without (closed circle) energy dissipation ($k = 2$ MPa).

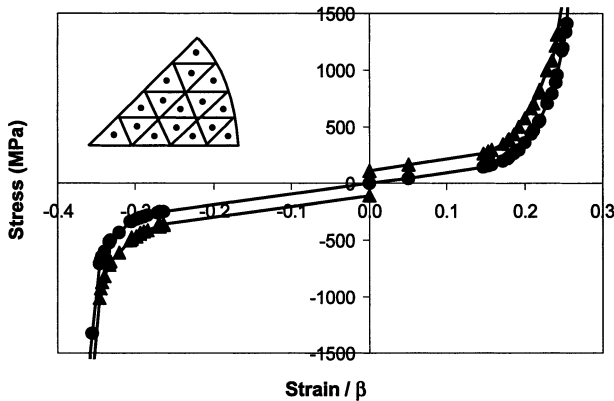


Fig. 5. Stress–strain curves of a polycrystal having 16 types of grains with (closed triangle) and without (closed circle) energy dissipation ($k = 2$ MPa).

Figs. 4 and 5 are for the cases of nine and 16 groups of grains, the cases including energy dissipation. From these results, we observe:

- 1) the increase in the number of grain groups from four to 16 does not significantly change the σ_0 versus ε relationship, except near the largest strain attained.
- 2) After an initial low gradient stage, the stress increases sharply as the strain approaches a limiting value. The largest strain regions are not fully shown in Figs. 3–5, because the effect of energy dissipation cannot be seen in the low strain regime, if the largest strain is plotted. For reference, we will simply quantify the largest stress attained: It is approximately 8×10^3 MPa in the four grain problem, 1.5×10^4 MPa in the nine grain problem and 2.7×10^4 MPa in the 16 grain problem.
- 3) The limiting (maximum) strain is about 0.27β in tension and about 0.37β in compression, regardless of the number of grain groups examined. These observations will be discussed in the next section.

3. Discussion

Observation (1) implies that four grain types are enough to estimate the σ_0 versus ε relationship in polycrystalline Fe–Pd. Even a model polycrystal having two types of grain groups has a very similar σ_0 versus ε relationship to those in Figs. 3–5, except in the large strain region.

In more detailed examination, observation (2) is better stated in the following manner. More stages exist after the first low slope regime. The origin of the existence of many stages having different slopes is most clearly demonstrated by examining an artificial polycrystal consisting of only one type of grain group, the problem which results in two stages. In the standard stereographic triangle:

$$l_2^2 \leq l_1^2 \leq l_3^2 \quad (31)$$

In this case, f_3^* monotonically decreases from 0 to $-1/3$ in the first stage, when the uniaxial stress is tensile. That is, in this stage BCV(3) disappears as strain increases. In the second stage having larger slope, f_2^* increases to $2/3$, while f_1^* decreases to $-1/3$. In this one type of grain problem, the elastic energy is written as:

$$W = \frac{1}{2} \alpha \beta^2 (f_1^{*2} + f_2^{*2} + f_3^{*2}) - \frac{3}{4} \alpha \beta^2 \{f_1^* l_1^2 + f_2^* l_2^2 + f_3^* l_3^2\}^2, \quad (32)$$

per unit volume, by putting $g(1) = 1$ in Eq. (22). The strain along the loading direction is given by Eq. (10). In the very beginning of the first stage,

$$\delta W = 0, \quad (33)$$

because $f_1^* = f_2^* = f_3^* = 0$. Thus, in the absence of energy

dissipation, the stress σ_0 needed to initiate straining at the start of the first regime becomes zero.

In the second stage, W is written as:

$$W = \frac{1}{2}\alpha\beta^2\left(f_1^{*2} + f_2^{*2} + \frac{1}{9}\right) - \frac{3}{4}\alpha\beta^2\left\{f_1^*l_1^2 + f_2^*l_2^2 - \frac{1}{3}l_3^2\right\}^2, \quad (34)$$

because,

$$f_3^* = -\frac{1}{3} \quad (35)$$

In this stage,

$$\delta f_1^* = -\delta f_2^* \quad (36)$$

Thus,

$$\delta W = \alpha\beta^2(f_2^* - f_1^*)\delta f_2^* - \frac{3}{2}\left(f_1^*l_1^2 + f_2^*l_2^2 - \frac{1}{3}l_3^2\right) \times (l_2^2 - l_1^2)\delta f_2^* \quad (37)$$

which is approximated to:

$$\delta W = \alpha\beta^2\delta f_2^* - \frac{3}{2}\left(\frac{l_2^2 + l_3^2}{3} + \frac{l_2^2 + l_1^2}{3}\right)(l_2^2 - l_1^2)\delta f_2^* \quad (38)$$

since

$$f_2^* \approx \frac{2}{3}, \quad f_1^* \approx -\frac{1}{3} \quad (39)$$

at the very end of the second stage. The stress σ_0 needed to supply this energy, Eq. (38), is calculated by $\sigma_0\delta\varepsilon$. $\delta\varepsilon$ is given as:

$$\delta\varepsilon = -(l_2^2 - l_1^2)\delta f_2^* \quad (40)$$

from Eq. (10). Thus, we obtain:

$$\sigma_0 = \alpha\beta\frac{1}{l_1^2 - l_2^2} + \alpha\beta((l_1^2 - l_2^2) + (l_3^2 - l_2^2)) \quad (41)$$

from Eqs. (38) and (40). This is significantly large. Note that $l_1^2 - l_2^2$ and $l_3^2 - l_2^2$ are positive in the standard triangle examined.

The stress in the last stage becomes larger as the number of grains increases; Eq. (2). This is also consistent with the above reasoning. As seen in Figs. 3–5, as the number of grain groups increases, more grains having the orientation near $\langle 111 \rangle$ are introduced. At the exact $\langle 111 \rangle$ orientation, l_2^2 becomes equal to l_1^2 . This means that the first term in Eq. (41) increases rapidly as the number of grain groups examined in the calculation increases. However, the large stress region near the end of complete variant change should not be emphasized so strongly. In reality, such large stress induces plastic deformation by dislocation movement, prior to the completion of the variant change. The

plastic deformation obscures the sharp rise in stress predicted theoretically in the present study.

Observation (3) shows that the present method to assign the volume fraction to each grain group is adequate to model a polycrystal consisting of grains having completely random orientations. Without elastic stress consideration, we can calculate the largest elongation as the average of the maximum strain achieved by all the grains. The strain of a grain is given by Eq. (10). In the standard stereographic triangle, l_2^2 is the smallest among all l_i^2 . This means that the maximum strain attained by the variant change occurs when f_2^* becomes $2/3$ and f_1^* and f_3^* become $-1/3$ (β is positive). Thus, the maximum strain of a grain is given by:

$$\varepsilon_{\max} = \beta\left(\frac{1}{3} - l_2^2\right) \quad (42)$$

The average of Eq. (42) over the standard triangle is calculated as $(2/\pi)(1 - 1/\sqrt{3})\beta = 0.2694\beta$, which agrees with the maximum strain observed by the calculation shown in Figs. 2–5. For compression, the corresponding expression is given by:

$$\varepsilon_{\max} = \beta\left(\frac{1}{3} - l_3^2\right) \quad (43)$$

The average of Eq. (43) over the standard triangle is $-2/(\sqrt{3}\pi)\beta = -0.368\beta$, which also agrees with the largest strain seen in Figs. 2–5.

Next, we would like to mention why the elastic energy is concisely written as in Eqs. (21) and (22). This is simply due to the assumption that grains having the same direction along the loading axis are present axisymmetrically with respect to the loading direction. Otherwise, such a simple expression as Eq. (12) cannot be obtained: i.e. the interaction energy W_I cannot be written as simply as in Eq. (21). This case of non-axisymmetric texture applies to a material having a sheet or plate texture. If a material has a fiber texture (axisymmetric texture), the present method results in an equally simple formulation of energy and the pre-determination of $l(I)$ and $g(I)$ in the fiber textures is all that is required to find the σ_0 versus ε relationship.

Some papers postulate that the direction of the magnetization vector of a magnetic domain in Fe–Pd martensite is determined by the type of BCVs [3,4,6–8]. Thus, they advocate that a magnetic field favors a certain variant over others and can control straining. If this is the case, straining in polycrystalline Fe–Pd by magnetic field should also be examined along the same lines as in the present study. However, a recent work by Yamamoto, Wang and Hirayama indicates that magnetic domains in Fe–Pd have no one-to-one correspondence to martensite variants [14]. Thus, we must examine magnetic field induced straining in more detail, as will be fully discussed in a separate paper.

Furuya et al. [6–8] have observed strain of the order of 0.1% by the application of a magnetic field to polycrystalline Fe–Pd, which is clamped at one end and loaded parallel to its length at the other end [6,7]. An Fe–Pd specimen is in a fully martensite state. Even though they have claimed that the strain is due to a direct effect of the magnetic field alone, we rather think that the strain is caused by force produced by a heterogeneous distribution of magnetic field, which induces the magnetic force. The force exerts bending moment to a specimen clamped at one end [15,16]. The moment results in stress, which, in turn, causes straining by variant change. One of their papers [7] has indicated that the sign of the strain changes, when an identical sheet specimen is rotated by about 180°. A sheet specimen is placed between two poles of an electromagnet. The direction of the field is normal to the surface of the specimen, upon which is mounted one strain gage. As reported previously [16], this geometry most likely induces force on a specimen, unless the specimen is exactly in the center of the field, where there is absolutely no gradient of the field. (Slight deviation in position causes force, which moves a magnetic material to the nearer pole and induces more force.) Thus, the 180° rotation changes the sign of strain measured on one surface. This reasoning indicates that 0.1% strain claimed by Furuya et al. to be pure magnetostriction is most likely rather due to stressing. When their specimen is rotated by 90°, the strain becomes much smaller. In this geometry, the specimen has the largest rigidity against bending caused by a heterogeneous magnetic field, resulting in small strain measured on a surface. We may further add that if the strains before and after the 180° rotation, observed by Furuya et al [7], are averaged, the averaged strain becomes 0.01%, which agrees with our own measurement [5]. The average for 180° rotation is equivalent to that of strains measured on two surfaces of the specimen, which is apt to bending by moment, to get tensile strain.

4. Summary

The change in the variants of martensite in an Fe–Pd polycrystal under uniaxial loading is formulated by evaluating the associated changes in elastic energy and potential energy of a loading device. The change in the variant fractions leads to straining and, thus, a uniaxial stress–strain relationship is computed. The energy dissipation needed for the movement of variant interfaces is also taken into account. The dissipation energy is estimated using a dislocation theory. Implications of the results are also discussed in relation to straining by the application of magnetic field.

Acknowledgements

This study was supported by DARPA-ONR contract (N-00014-00-1-0520). Dr E. Garcia of DARPA and Dr R. Barsoum of ONR are the program monitors. Further support was given by a NEDO grant on Smart Materials where Dr A. Sakamoto is the program monitor.

Appendix A

Consider a grain, the orientation of which is produced by the rotation of 180° around the loading direction of the grain whose eigenstrain is written in Eq. (8). The eigenstrain of the former grain is written as:

$$\varepsilon^*(I, x) = -\beta \begin{bmatrix} \lambda_1(I) & \varepsilon_{12}^*(I) & -\varepsilon_{13}^*(I) \\ -\varepsilon_{21}^*(I) & \lambda_2(I) & -\varepsilon_{23}^*(I) \\ -\varepsilon_{31}^*(I) & -\varepsilon_{32}^*(I) & \lambda_3(I) \end{bmatrix} \quad (\text{A.44})$$

That is, the {13} and {23} components in Eqs. (8) and (A.44) cancel out. This cancellation applies to those other grains belonging to the I -th group, since all these grains are axisymmetrically present with respect to the loading direction.

Instead of 180°, consider rotation of 90°. A grain in this new orientation has the eigenstrain of:

$$\varepsilon^*(I, x) = -\beta \begin{bmatrix} \lambda_2(I) & -\varepsilon_{12}^*(I) & -\varepsilon_{23}^*(I) \\ -\varepsilon_{21}^*(I) & \lambda_1(I) & \varepsilon_{13}^*(I) \\ -\varepsilon_{23}^*(I) & -\varepsilon_{31}^*(I) & \lambda_3(I) \end{bmatrix} \quad (\text{A.45})$$

Thus, the {1,2} component of eigenstrain in a grain having Eq. (8) and in that having Eq. (A.45) cancel out.

By any rotation around the loading direction, the sum of the {1,1} and {2,2} components are constant and the {3,3} component does not change. In this way, the average eigenstrain of the grains belonging to the I -th group is obtained as:

$$\begin{aligned} \langle \varepsilon^*(I, x) \rangle_{V_0} \\ = -\beta \begin{bmatrix} (\lambda_1(I) + \lambda_2(I))/2 & 0 & 0 \\ 0 & (\lambda_1(I) + \lambda_2(I))/2 & 0 \\ 0 & 0 & \lambda_3(I) \end{bmatrix} \end{aligned} \quad (\text{A.46})$$

From this, we obtain (Eq. (12)), using ([11]).

Appendix B

Here, we discuss the stress needed for an interface between two BCVs to move. Since two adjoining BCVs match perfectly on their interface, the movement is caused by the nucleation of a dislocation loop on the interface and its subsequent spreading-out. Apparently, nucleation is the rate controlling process. The energy change when a dislocation loop is formed (Gibbs free

energy assigned for the loop) is approximately written as:

$$G = 2\pi r \frac{1}{2} \mu b^2 - \sigma_0 \pi r^2 b, \quad (\text{A.47})$$

where b is the Burgers vector of the dislocation and r the radius of the loop. The maximum of G (activation energy) is calculated as:

$$G^* = \frac{\pi \mu^2 b^3}{(4\sigma_0)}. \quad (\text{A.48})$$

As often used in dislocation dynamics, such a process occurs with an observable rate, when:

$$G^* = 26k_B T, \quad (\text{A.49})$$

where k_B is the Boltzmann constant and T the temperature [17]; b in this case is in the order of $a_0(\varepsilon_a - \varepsilon_c)$; a_0 is taken as the lattice parameter of the austenite). Using $T = 300$ K, $a_0 = 0.375$ nm, $(\varepsilon_a - \varepsilon_c) = 2.54 \times 10^{-2}$ and $\mu = 15$ GPa, Eqs. (A.48) and (A.49) give:

$$\sigma_0 = 1.4 \text{ MPa} \quad (\text{A.50})$$

as the stress for the interface movement. Note that σ_0 has the same meaning as k in Eq. (29). Thus, the magnitude of the adopted value of $k = 10^{-4} \mu$ has been successfully explained.

An interface which is not perfectly flat in the beginning contains steps. The steps are dislocations as discussed here. When they move, they eventually disappear at a specimen surface or a grain boundary or annihilate each other. This process leads to micro-straining. After this process, an interface becomes flat. Long distance movement of a variant interface, leading to large strain, requires the process discussed in the above paragraph. Since flat interfaces are crystallographically fixed, one cannot control the mobility of the interfaces for long distance movement as one wishes.

Usual grain boundaries do not play any role in this movement. This means that such a proposal as advocated by [7] to modify boundaries and interfaces to get larger straining makes no sense in the actual straining of Fe–Pd by variant change.

References

- [1] H. Kato, Y. Liang, M. Taya, *Scripta Mater.* 46 (2001) 471.
- [2] M. Kato, T. Wada, Y. Liang, T. Tagawa, M. Taya, T. Mori, to appear in *Mater. Sci. Eng. A*.
- [3] R.D. James, M. Wuttig, *Phil. Mag. A* 77 (1998) 1273.
- [4] J. Koeda, Y. Nakamura, T. Fukuda, T. Kakeshita, T. Takeuchi, K. Kishio, *Trans. Mater. Res. Soc. Jpn.* 26 (2001) 215.
- [5] Y. Liang, T. Wada, M. Taya and T. Mori, *Acta Metall.*, submitted.
- [6] Y. Fumya, T. Watanabe, N. Hagood, H. Kimura, J. Tani, in: N.W. Hagood, M.J. Atalla (Eds.), *Proceedings 9th International Conference on Adaptive Structures and Technologies*, Technomic, 1998, p. 271.
- [7] T. Onogi, Y. Furuya, S. Tsurekawa, T. Watanabe, *Proceedings Mechanical Engineering Congress*, vols. 99-1, Japan Society of Mechanical Engineers, 1999, p. 293.
- [8] Y. Fumya, N. Hagood, H. Kimura, T. Watanabe, *J. Magn. Soc. Jpn.* 23 (1999) 400.
- [9] T. Mori, K. Tanaka, *Acta Metall.* 21 (1973) 571.
- [10] L.M. Brown, *Acta Metall.* 21 (1973) 879.
- [11] T. Mura, *Micromechanics of Defects in Solids*, Martinus Nijhoff, 1987, p. 79.
- [12] T. Tagawa, T. Wada and M. Taya, to appear in *Scripta Mater.*
- [13] R. Oshima, *Scripta Metall.* 15 (1981) 829.
- [14] K. Yamamoto, Z. Wang, T. Hirayama, *Proceedings of 57th Annual Meeting, Japan Society of Electron Microscopy*, 2001, p. 179.
- [15] Y. Liang, H. Kato, M. Taya, *Proceedings Plasticity '00:8th International Symposium, Plasticity and Current Applications*, Whistler, 2000, p. 193.
- [16] Y. Liang, H. Kato, M. Taya, T. Mori, *Scripta Mater.* 45 (2001) 569.
- [17] E. Kuramoto, Y. Aono, Y. Kitajima, K. Maeda, S. Takeuchi, *Phil. Mag. A* 39 (1979) 717.